Applied Catalysis A: General 367 (2009) 122–129

Contents lists available at ScienceDirect

Applied Catalysis A: General

journal homepage: www.elsevier.com/locate/apcata

Deactivation and regeneration of Cu/SiO_2 catalyst in the hydrogenation of maleic anhydride. Kinetic modeling

Camilo I. Meyer [a], Alberto J. Marchi [a], Antonio Monzon [b], Teresita F. Garetto [a,*]

[a] Catalysis Science and Engineering Research Group (GICIC), INCAPE, UNL-CONICET, Santiago del Estero 2654, 3000 Santa Fe, Argentina
[b] Department of Chemical and Environmental Engineering, Faculty of Science, University of Zaragoza, 50009 Zaragoza, Spain

ARTICLE INFO

Article history:
Received 16 April 2009
Received in revised form 24 July 2009
Accepted 28 July 2009
Available online 5 August 2009

Keywords:
Deactivation
Kinetic modeling
Selective hydrogenation
Maleic anhydride
Copper-based catalysts

ABSTRACT

In this work, the deactivation of a $Cu(10\%)/SiO_2$ catalyst in the gas-phase hydrogenation of maleic anhydride (*MA*) was studied. The reaction was performed between 170 and 220 °C, at atmospheric pressure and using two contact times (W/F^0_{MA}): 11.9 and 23.8 g cat. h/mol *MA*. The $Cu(10\%)/SiO_2$ catalyst was prepared by the wetness impregnation method and characterized by N_2 physisorption at −196 °C, N_2O decomposition at 90 °C, X-ray diffraction and temperature programmed reduction. From this characterization, it was concluded that catalyst is formed by large metal copper crystallites with little or none interaction with silica surface. Under the conditions used in this work, the $Cu(10\%)/SiO_2$ catalyst was highly selective to succinic anhydride (*SA*) while *MA* conversion dropped drastically with time. Both high selectivity to *SA* and rapid catalyst deactivation can be explained considering different types of *MA* interaction with the large metal copper crystallites. Catalyst regeneration feasibility under two different atmospheres, oxidizing and reducing, was also analyzed. The experimental results were successfully fitted, by non-linear regression, using a deactivation model with residual activity (*DMRA*). This model predicts satisfactorily the deactivation of $Cu(10\%)/SiO_2$ in the gas-phase hydrogenation of *MA*, both for fresh and regenerated catalysts, under the experimental conditions used in this work.

1. Introduction

The global reaction network for maleic anhydride (*MA*) hydrogenation is shown in Fig. 1. In this process, both hydrogenation and hydrogenolisis reactions are involved. Some of the reaction products, succinic anhydride (*SA*), γ-gammabutyrolactone (*GBL*), tetrahydrofurane (*THF*), and 1,4 butanediol (*BDO*), are important starting materials in chemical industry in order to obtain polymers, pharmaceutical compounds and additives. In particular, *SA*, the first product in the reaction sequence, is widely used in the manufacture of polymeric materials, pharmaceuticals, agrochemicals, dyes, photographic chemicals, surface active agents, lubricant additives, organic flame retardant materials, esters, flavors and fragrances.

In the open literature, several papers reported different type of catalysts and a variety of operating conditions in order to carried out the *MA* hydrogenation [1–15]. The reaction was studied using several types of noble metal-based catalysts, such as Pd, Pt, Au [4,9–13], both in liquid phase and gas phase [12–14]. Generally, the experiments were carried out in the temperature and pressure ranges of 190–240 °C and 1–5 MPa, respectively. Copper-based catalysts were also used to study the gas-phase hydrogenation of *MA* between 210 and 280 °C [5,15]. In general, the catalysts composition of these copper-based catalysts is rather complex since, besides copper, other elements are included, as for instance, Al, Zn, Cr and Ce. But the use of noble metal and polluting chromium in the catalyst is unfavorable in view of both catalyst cost and environmental protection. In all of the cases, the main products reported were *SA*, *GBL*, *THF* and *BDO*. Depending on the reaction conditions and the type of catalyst, the product distribution was different. Other less valuable by-products may also be obtained during *MA* hydrogenation, such as propionic acid (PA), methane and CO [7,8]. In some cases, partial catalyst deactivation has been reported for copper-based catalysts [15]. At the present time, no satisfactory explanations for this deactivation have been given. In this work, we analyze the behavior of a $Cu(10\%)/SiO_2$ catalysts during selective *MA* hydrogenation in gas phase with the objective to determine the possible deactivation causes as well as the possibility of the catalyst regeneration. A kinetic modeling was carried out in order to obtain additional information to explain the observed deactivation. A deactivation model with residual activity (*DMRA*) was used to fit the experimental data considering both differential and integral operation of the reactor. On the basis of the obtained results, a mechanistic model is postulated to explain the selective *MA* hydrogenation and the deactivation-regeneration process.

* Corresponding author. Tel.: +54 342 4533858; fax: +54 342 4531068.
E-mail address: tgaretto@fiq.unl.edu.ar (T.F. Garetto).

0926-860X/$ – see front matter © 2009 Elsevier B.V. All rights reserved.
doi:10.1016/j.apcata.2009.07.041

Nomenclature

a	activity
C_{MA}	concentration of maleic anhydride
d	kinetic order in the deactivation term of the net deactivation rate
d_m	kinetic order in the regeneration term of the net deactivation rate
E_a	apparent activation energy for maleic anhydride hydrogenation
E_d	apparent activation energy for the deactivation stage
E_r	apparent activation energy for the regeneration stage
F^0_{MA}	Molar flow rate of maleic anhydride
h	number of active sites involved in the controlling step of the side reaction responsible for the deactivation.
k	kinetic constant rate
k_d	intrinsic kinetic constant of deactivation
k_r	intrinsic kinetic constant of regeneration
m_1	kinetic order respect to H_2
n_1	kinetic order respect to maleic anhydride
m_d, n_d	kinetic orders with respect to maleic anhydride and H_2 for Ψ_d
m_r, n_r	kinetic orders with respect to maleic anhydride and H_2 for Ψ_r
m	number of active sites involved in the controlling step of the main reaction, hydrogenation of maleic anhydride
p_{H_2}	partial pressure of H_2
p_{MA}	partial pressure of maleic anhydride
R	ideal gas constant (1.9859 cal K^{-1} mol^{-1})
$(-r_{MA})_0$	initial reaction rate
$(-r_{MA})_t$	reaction rate at time t
T	temperature
t	time
W	mass of catalytic bed
X_{MA}	conversion of maleic anhydride
$(X_{MA})_0$	initial conversion of maleic anhydride
$(X_{MA})_t$	conversion of maleic anhydride at the time t
z	reactor position
ε_B	bed porosity
ρ_B	bed density
ψ_d	deactivation kinetic function
ψ_r	regeneration kinetic function
ψ_G	global kinetic function
μ	fluid viscosity

2. Experimental

2.1. Catalyst preparation and characterization

A Cu/SiO_2 catalyst, 10% in copper, was prepared by incipient-wetness impregnation of SiO_2 powder (Grace G62, 99.7%, Na: 0.1%, SO_4^{2-}: 0.1%, others: 0.1%) at 30 °C and using an aqueous solution of $Cu(NO_3)_2$ (0.66 M). The impregnated silica was dried at 120 °C for 24 h and then calcined in air at 500 °C for 2 h. Copper loading was verified by using atomic absorption spectroscopy.

The specific surface area of the oxide precursor, after impregnation and calcination, was measured by N_2 physisorption at −196 °C using a Quantachrome Autosorb-1 sorptometer and BET analysis methods. Sample was degassed at 250 °C before carrying out the analysis.

The reducibility of the copper oxide species was determined by temperature programmed reduction (TPR) using a Micromeritics AutoChem 2920, with a thermal conductivity detector. TPR profile was obtained in a 5%H_2/Ar gas stream (60 cm^3/min STP) while the temperature was increased from 25 to 500 °C at 10 °C/min. The exit gas from the reactor was passed through a cold trap at −70 °C, before entering to the thermal conductivity detector, with the aim to remove the water formed during sample reduction.

XRD data was recorded at 30 °C by employing a Shimadzu D-1 diffractometer using Cu-Kα radiation (λ = 1.5418 Å) and a Ni filter. Analysis was carried out using a continuous scan mode at 2°/min over a 2θ range of 10–80°. Crystallite medium size was calculated from the CuO (1 1 1) diffraction line applying Debye-Scherrer equation.

Metal copper dispersion was determined by N_2O decomposition a 90 °C and the evolution of the surface reaction products was measured by mass spectrometry in a Balzers Omnistar unit. The sample was reduced in situ at 300 °C, prior feeding N_2O. Afterwards, sample was exposed to pulses of N_2O(10%)/Ar. The stoichiometry was assumed to be $Cu^0_{sup}/N_2O = 2$, where Cu^0_{sup} is a copper atom on surface.

2.2. Catalytic activity

The gas-phase hydrogenation of *MA* was carried out at atmospheric pressure in a flow set-up equipped with a fixed-bed tubular reactor (SS 1.5 cm i.d.). Samples were pressed to obtain tablets that were then crushed and screening. The fraction in the range of 0.35–0.42 mm was loaded to the reactor after dilution with quartz using a quartz/catalyst ratio of 1. Catalyst loadings (W) of 0.050 and 0.100 g, contact times (W/F^0_{MA}) of 11.9 and 23.8 g cat. h/mol *MA* and gas flow rate of 150 cm^3 min^{-1} were used for the catalytic tests. In all cases, the catalytic tests were carried out at 170, 180, 195, 210 and 220 °C. Catalyst bed temperature was measured and controlled using a J-type thermocouple and a PID controller-programmer. Before activity tests, the catalyst sample was reduced in H_2 flow (100 cm^3 min^{-1}) at 300 °C for 1 h. Gas stream at the reactor outlet was analyzed by on-line gas chromatography using a Varian CP 3380 equipped with a flame ionization detector and a Graphpac GC 0.1% AT-1000 (80–100) packed column. It was verified that diffussional limitations do not alter the reaction rate measurements by carrying out experiments varying particle size and contact time between 0.15–0.60 mm and 10–80 g cat. h mol^{-1}, respectively.

After catalytic test, coke content on the used catalyst samples was determined by temperature programmed oxidation (TPO) measurements. TPOs were obtained in a flow set-up by heating the sample from room temperature to 600 °C, at 10 °C/min, in a O_2(1%)/N_2 gas stream. The evolved CO_2 was converted to CH_4 over a Ni(40%)/Kieselghur catalyst at 400 °C. The methanator outlet was monitored using a flame ionization detector (FID). Data acquisition was carried out by using Peak 356 software. Calibration was made with pattern catalyst having an amount of coke well known.

3. Results and discussion

3.1. Catalyst characterization

The textural analysis of Cu(10 wt%)/SiO_2 catalyst gave a specific surface area (Sg) of 232 m^2 g^{-1}, a pore volume (Vp) of 0.903 cm^3 g^{-1} and a pore diameter (Dp) of 139 nm. The SiO_2 used

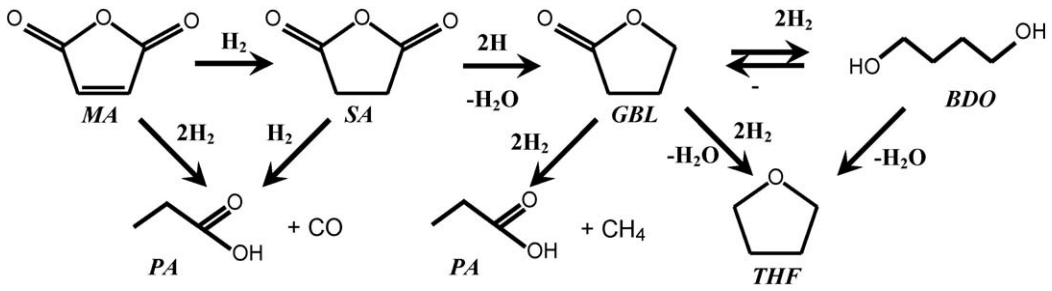

Fig. 1. Reaction network for maleic anhydride hydrogenation over metal catalysts.

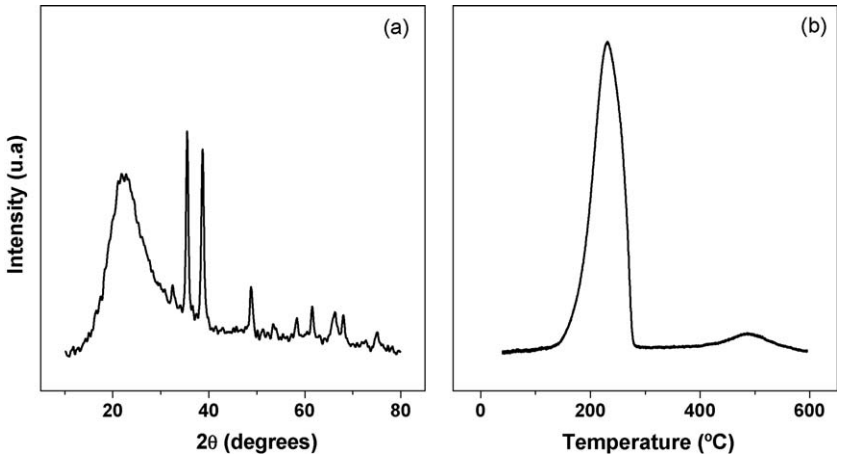

Fig. 2. Characterization of Cu(10%)/SiO_2 after calcination at 500 °C, (a) XRD pattern, (b) TPR profile.

as support has Sg = 253 $m^2\,g^{-1}$, Vp = 0.88 $cm^3\,g^{-1}$ and Dp = 139 nm. These results are indicating that the impregnation method did not modify substantially the textural properties of the support.

The X-ray diffraction (XRD) pattern corresponding to Cu(10%)/SiO_2 sample after thermal treatment is shown in Fig. 2a. The main two peaks were observed at $2\theta = 35.4^\circ$ and $2\theta = 38.5^\circ$. This diffractogram is consistent with JCPDS data assigned to a monoclinic copper oxide phase (JCPDS 41-254). Besides, this copper oxide phase is formed by large crystallites with a medium size of about 21 nm. The metallic dispersion of Cu/SiO_2 catalyst determined by N_2O decomposition gave a value of 2.2%. This value is indicating that metallic phase is also formed by large particles of metal copper. These results are in agreement with the fact that the large particles of metal copper are coming from the reduction of large crystallites of CuO.

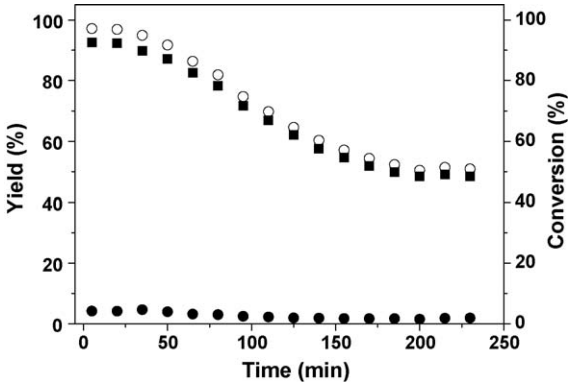

Fig. 3. Gas-phase hydrogenation of maleic anhydride (*MA*) on Cu(10%)/SiO_2 at 220 °C (P = 1 bar, $W/F^0_{MA} = 23.8\,g\,cat.\,h/mol\,MA$); (○) *MA* conversion; (■) yield to succinic anhdydride; (●) yield to γ-butyrolactone.

The temperature programmed reduction profile of the CuO/SiO_2 sample is presented in Fig. 2b. This reduction profile shows only one reduction peak with a maximum H_2 uptake at 230 °C. This peak may be assigned to the reduction of CuO to Cu^0. Besides, in agreement with the XRD analysis, the peak is asymmetric and wide which is indicative that large crystallites of CuO are involved in the reduction process [16].

3.2. Catalytic results

In all cases, the only products detected and analyzed were *SA* and *GBL*. As a representative example, the evolutions of the *MA* conversion and the *SA* and *GBL* yields with time, for the catalytic test at 220 °C and $W/F^0_{MA} = 23.8\,g\,cat.\,h/mol\,MA$, are shown in Fig. 3. As it can be seen, the catalyst is highly selective to convert *MA* into *SA*. *GBL* yields were always lower than 2–3% in all cases. Then, it is also clear that the evolution of the *SA* yield with time follows the same trend as the *MA* conversion.

Fig. 4 shows the evolution of the *MA* conversion with time at different temperatures in the 170–220 °C range and for $W/F^0_{MA} = 11.9\,g\,cat.\,h/mol\,MA$. In all cases, the conversion diminishes and reaches a residual activity after 2–4 h of reaction. When the reaction temperature was raised from 170 to 220 °C, the initial conversion increased from 20 to 100%. Similarly, the residual conversion increases from 5% to 60%. At 220 °C the AS yield was higher than 97% and at lower reaction temperatures it was always 100%.

In order to determine if the observed deactivation may be attributed to coke deposition, after catalytic test at 220 °C and $W/F^0_{MA} = 23.8\,g\,cat.\,h/mol\,MA$, a TPO analysis of the used catalyst was carried out. A broad O_2 consumption peak with a maximum at 260 °C was observed (not shown). This TPO signal could correspond to oxidation of coke precursors deposited on the catalyst surface. However, it cannot be ruled out that some species

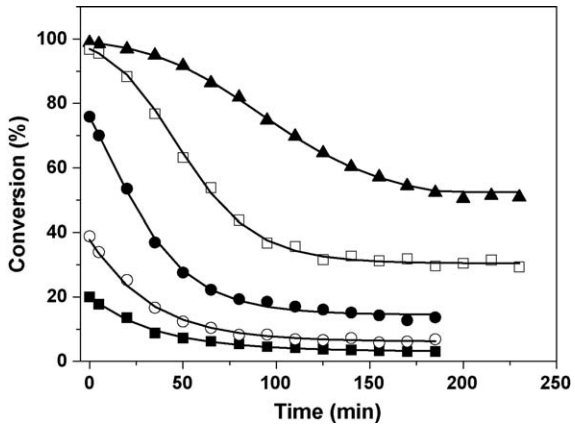

Fig. 4. Maleic anhydride (*MA*) conversion over Cu(10%)/SiO_2 at different temperatures (W/F^0_{MA} = 11.9 g cat. h/mol *MA*). Experimental data: 170 °C (■), 180 °C (○), 195 °C (●); 210 °C (□), 220 °C (▲). Modeling: full lines.

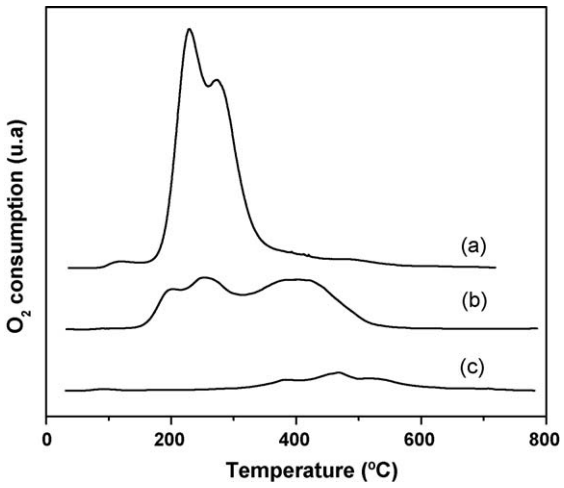

Fig. 6. TPO profiles of Cu(10%)/SiO_2 catalyst after reaction at 170 °C (a), after H_2 regeneration (b) and after air regeneration (c).

involved in the reaction remains irreversibly adsorbed on metal copper surface. Then, they could also be responsible for the deactivation observed. The amount of deposited carbon determined by TPO for this sample was 2.4%.

3.3. Regeneration experiments

In order to determine if the observed deactivation is reversible or irreversible, we tried two regeneration procedures of the catalyst after reaction: (i) treatment in H_2(100%) at 300 °C for 3 h and (ii) treatment in air at 300 °C for 2 h, followed by reduction in H_2(100%) at 300 °C for 1 h. Afterwards, the fresh and regenerated catalysts were tested in the gas-phase *MA* hydrogenation at 170 °C and W/F^0_{MA} = 11.9 g cat. h/mol *MA*. Fig. 5a shows the evolution of *MA* conversion with time for fresh catalyst and after treatment (i). It can be observed that the initial *MA* conversion with catalyst regenerated in H_2 was lower than the initial conversion with the fresh catalyst. Instead, the initial conversion with the catalyst regenerated in air is some higher than the initial conversion with fresh catalyst (Fig. 5b). The residual conversion after 3 h reaction was similar in all of the cases (Fig. 5). In short, these results are indicating that the deactivation process could be similar in all the cases, i.e. with the regenerated and fresh catalysts.

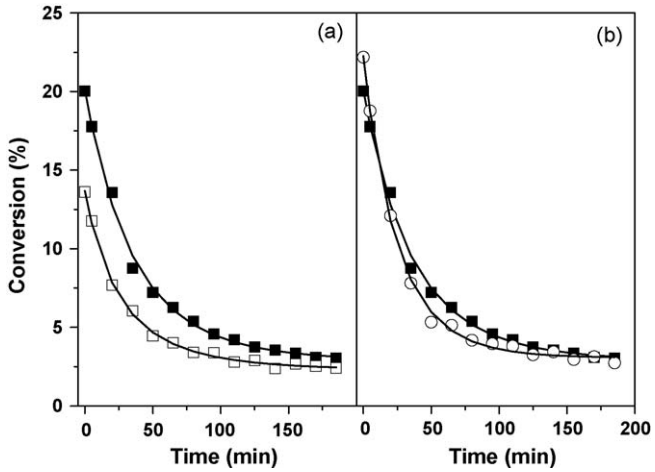

Fig. 5. Gas-phase hydrogenation of maleic anhydride (*MA*) over Cu(10%)/SiO_2 at 170 °C (W/F^0_{MA} = 11.9 g cat. h/mol *MA*). Experimental data: (a) fresh catalyst (■); H_2 treatment at 300 °C (□); (b) fresh catalyst (■); air treatment at 300 °C (○). Modeling: full lines.

In order to obtain more information on the deactivation-regeneration process some additional TPO experiments were carried out (Fig. 6). For fresh Cu/SiO_2 catalyst, two peaks with maxima at about 230 and 275 °C were observed (curve a). The amount of deposited carbon determined by TPO was 1.1%. After treatment in H_2, (curve b) the peaks observed in the TPO profile were less intense and the maxima were at 260 and 410 °C, approximately. Quantification of the remaining carbon gave about 0.6%. Instead, after regeneration in air, the measured remaining carbon was less than 0.1% (curve c). These results are consistent with the trend observed for the catalytic experiments (Fig. 5).

TPO results are indicating that some of the carbon species, deposited on the catalyst surface during gas-phase *MA* hydrogenation, remains after H_2 treatment. Moreover, some of the coke precursors changed to a more stable state during H_2 treatment. Then, the activity is only partially recovered and the initial conversion is lower than with the fresh catalyst. Instead, after treatment in air flow, practically all the carbon species are removed from the catalyst surface. Then, the initial activity was totally recovered. Actually, the initial conversion of catalyst treated in air was some higher than initial activity of fresh catalyst. Thus, some surface reconstruction of metal copper surface cannot be ruled out [16].

According to these results we assume that at least two types of carbonaceous species coexist on the catalyst surface after reaction: one of them can be removed by treatment in H_2 flow at 300 °C, but the other one is removed only after treatment in air at the same temperature. A plausible explanation is that these deactivating species are unsaturated compounds (for instance, the *MA* itself and/or some coke precursor) strongly adsorbed, having different degrees of interaction with the catalyst surface.

In order to get a further comprehension on the deactivation-regeneration process, a kinetic modeling of the catalytic system was carried out.

3.4. Deactivation kinetic model with residual activity (DMRA)

During a deactivation process, the catalyst may be totally deactivated or it may reach a certain residual activity level. In the latter case, the residual activity may be ascribed to one or more causes, for example: (1) nature of the active sites, (2) the reaction mixture composition, (3) the deactivation mechanism, (4) reversible or irreversible coke deposition. It is then necessary to

use more complex kinetic models than the conventional ones to get an adequate prediction of the catalyst behavior during operation time. Kinetic deactivation models that take into account the above aspects have been previously developed [17–24]. These models are based on reaction-deactivation mechanisms that can theoretically predict the presence of residual activity. In the present case, it must also be considered that there is a significant excess of hydrogen in the reaction medium. We assumed that this hydrogen can react with the coke precursors adsorbed on the catalyst surface to regenerate it, at least partially. The last could account for, at least in part, the catalyst residual activity and how this residual activity is a function of the operation conditions [22–29].

The flow in the catalytic fixed-bed reactor, used in this work for activity tests, was assumed to be plug-flow type. In addition, it was supposed that neither radial nor axial dispersion of reactive exist in the catalytic bed. In these conditions, the mass balance corresponding to *MA* is given by Eq. (1).

$$-u\frac{\partial C_{MA}}{\partial z}-\rho_B\left(\frac{1-\varepsilon_B}{\varepsilon_B}\right)\cdot(-r^*_{MA})_t=\frac{\partial C_{MA}}{\partial t} \tag{1}$$

Assuming that the porosity (ε_B) and the bed density (ρ_B) are approximately constants, the initial reaction rate may be rewritten as:

$$(-r_{MA})_t=\rho_B\left(\frac{1-\varepsilon_B}{\varepsilon_B}\right)\cdot(-r^*_{MA})_t \tag{2}$$

Applying Eq. (2) and assuming pseudo-steady state approach, the mass balance given in Eq. (1) becomes:

$$\frac{\partial X_{MA}}{\partial(W/F^0_{MA})}=(-r_{MA})_t=(-r_{MA})_0\cdot a(t) \tag{3}$$

where $(-r_{MA})_0$ is the initial reaction rate and $a(t)$ is the catalyst activity, which is time-dependant.

Considering that the kinetic of the main reaction may be expressed by a power-law model, we can express $(-r_{MA})_0$ as:

$$(-r_{MA})_0=k_0\cdot p^{n_1}_{MA}\,p^{m_1}_{H_2} \tag{4}$$

In this study, the H_2/MA molar ratio was kept constant and equal to 130, high enough to consider that p_{H_2} is approximately constant. Then, we may define:

$$k_{MA}=k_0\cdot p^{m_1}_{H_2} \tag{5}$$

Then, with Eq. (5) in Eq. (4), the initial reaction rate may be expressed as a function of temperature and conversion as follows:

$$\begin{aligned}&(-r_{MA})_0=k_{MA}\,p^{n_1}_{MA}=k_{MA}\,p^{n_1}_{MA_0}(1-X_{MA})^{n_1};\\&k_{MA}=k_{MA_0}\exp(-E_a/RT)\end{aligned} \tag{6}$$

The parameter E_a is the apparent activation energy of the *MA* hydrogenation reaction. Considering the large excess of hydrogen during the reaction, the molar variation effect was neglected in this analysis.

According to the catalytic activity results (Figs. 3 and 4), a reversible coke-forming mechanism was assumed [20,22,27,28]. Then, the net deactivation rate can be obtained from the Eq. (7).

$$\frac{\partial a}{\partial t}=\psi_r\cdot a-\psi_r\cdot a^{d_m}-\psi_d\cdot a^d \tag{7}$$

The parameters ψ_d and ψ_r are the deactivation and regeneration kinetic functions, respectively. These kinetic functions include the influence of the operation conditions on the rate of deactivation. Thus, if power-law dependence is also assumed for both kinetic functions, the following expressions may be written:

$$\psi_d=k_d\,p^{n_d}_{MA}=k_d\,p^{n_d}_{MA_0}(1-X_{MA})^{n_d};\quad k_d=k_{d_0}\exp(-E_d/RT) \tag{8}$$

$$\psi_r=k_r\,p^{m_r}_{H_2}\cong const.;\quad k_r=k_{r_0}\exp(-E_r/RT) \tag{9}$$

Parameters k_d and k_r are the intrinsic kinetic constants for deactivation and regeneration, respectively. E_d and E_r are the apparent activation energies of the same deactivation and regeneration stages. The parameters n_d and m_r are the kinetic orders respect to *MA* and H_2, for ψ_d and ψ_r, respectively. Finally, the kinetic orders d and d_m, see Eq. (7), are depending on the number of active sites involved in the main reaction and deactivation process [27,28]. This dependence is given by:

$$d=\frac{m+h-1}{m};\quad d_m=\frac{m-1}{m} \tag{10}$$

The term m represents the number of active sites involved in the controlling step of the main reaction, i.e. *MA* hydrogenation. In a similar way, h stands for the number of active sites involved in the controlling step of the side reaction responsible for the catalyst deactivation [30].

In summary, the mathematical description for a reactor operating at high conversions, i.e. an integral reactor, is given by a set of two partial differential equations of first order, see Eqs. (2) and (7), which must be solved numerically. The boundary conditions for this equation system are:

$$\begin{aligned}&\forall\, t:\quad W/F^0_{MA}=0;\quad X_{MA}=0\\&\forall\, W/F^0_{MA}:\quad t=0;\quad a=1\end{aligned} \tag{11}$$

Therefore, for an integral reactor, the intrinsic kinetic parameters to be estimated are: k_{MA0}, E_a, k_{d0}, E_d, n_d, k_{r0} and E_r.

In the particular case of differential reactor operation, i.e. low *MA* conversion, the operating conditions are approximately constant along the reactor. Then, the mathematical model can be simplified assuming that the initial reaction rate $(-r_{MA})_0$ and the deactivation and regeneration kinetic functions, ψ_d and ψ_r, are constants along the reactor. In this situation, the reaction rate and the catalyst activity are directly calculated as:

$$(-r_{MA})_t=\frac{(F_{MA})_0}{W}(X_{MA})_t \tag{12}$$

$$a(t)=\frac{(-r_{MA})_t}{(-r_{MA})_0}=\frac{(X_{MA})_t}{(X_{MA})_0};\quad (X_{MA})_t=(X_{MA})_0\cdot a(t) \tag{13}$$

Since ψ_d and ψ_r are constants for differential reactor, Eq. (7) can be directly integrated for prefixed integer values of m and h. Thus, integrating Eq. (7) and substituting in Eq. (13), explicit algebraic expressions of the following type may be obtained:

$$(X_{MA})_t=\varphi\left[(X_{MA})_0,\psi_d,\psi_r,t\right] \tag{14}$$

Similar expressions have been deduced for other reaction systems [23,29]. Therefore, the only kinetic parameters that can be estimated from the experimental data, X_{MA} in function of time, for the case of differential reactor are ψ_d, ψ_r and $(X_{MA})_0$. In our particular case, differential operation of the reactor was possible only at 170 °C and $W/F^0_{MA}=11.9\,\mathrm{g\,cat.\,h/mol^{-1}}$. A fitting using a mathematic expression of the type shown in Eq. (14), which depends on the integer values of m and h, was carried out with the experimental data obtained under differential operation of the reactor. Only values with a real physical meaning for m and h, i.e. 1 or 2, were considered for these fittings. In fact, cases involving 3 or more active centers in an elemental step were not considered since they are quite improbable [31]. This assumption gives four different cases, which are shown in Table 1.

Table 1
Kinetic and statistical parameters obtained assuming differential operations for the hydrogenation reactor (T = 170 °C, W/F^0_{MA} = 11.9 g cat. h/mol *MA*, P = 1 bar).

m	h	$(X_{MA})_0$	ψ_d (min^{-1}) × 10^2	ψ_r (min^{-1}) × 10^3	SSR
Fresh catalyst					
1	1	20.0 ± 0.3	2.30 ± 0.101	4.3 ± 0.42	1.603
1	2	20.5 ± 0.4	3.38 ± 0.170	0	2.882
2	1	20.1 ± 0.3	2.45 ± 0.113	14.9 ± 1.37	1.487
2	2	20.3 ± 0.3	2.77 ± 0.150	4.8 ± 1.03	1.769
H_2 regeneration					
1	1	13.5 ± 0.2	2.74 ± 0.111	6.50 ± 0.43	0.607
1	2	13.8 ± 0.2	4.04 ± 0.168	1.10 ± 0.18	0.440
2	1	13.6 ± 0.2	2.98 ± 0.105	22.2 ± 1.15	0.399
2	2	13.7 ± 0.1	3.40 ± 0.110	10.0 ± 0.66	0.300
Air regeneration					
1	1	22.2 ± 0.3	3.34 ± 0.120	5.60 ± 0.4	1.180
1	2	22.7 ± 0.5	5.19 ± 0.390	0.40 ± 0.3	3.557
2	1	22.3 ± 0.3	3.61 ± 0.130	20.9 ± 2.1	1.119
2	2	22.5 ± 0.3	4.20 ± 0.130	7.60 ± 1	1.708

SSR: sum of square residuals.

It can be seen that the sum of square residuals (SSR column) was minimum when m = 2 and h = 1 (Table 1). However, a more or less close sum of square residuals (SSR) was obtained for $m = h = 1$. In order to get more certainty that the best fitting corresponds to the case when m = 2 and h = 1, we carried out an additional analysis fitting the m and h values, besides ψ_d, ψ_r and $(X_{MA})_0$. The estimates for m and h were 2.3 and 0.7, respectively. These estimates are closer to the pair m = 2 and h = 1 than to any of the other three cases. This result is in agreement with the fact that the best fitting was obtained for m = 2 and h = 1.

Experimental data obtained after treatment of used catalyst in H_2 and air were also fitted with the *DMRA* model assuming differential reactor operation, i.e. using Eq. (14). For the used catalyst treated in H_2 at 300 °C, the best fitting was obtained for $m = h = 2$ (Table 1, Fig. 5a). Instead, after regeneration in air at 300 °C, the best fitting was obtained when m = 2 and h = 1 (Table 1, Fig. 5b), similarly to fresh catalyst. In addition, the predicted initial conversion $(X_{MA})_0$ after regeneration in H_2 is some lower than $(X_{MA})_0$ for fresh catalyst. Instead, the model can predict that $(X_{MA})_0$ for catalyst regenerated in air is some higher than the one obtained with fresh catalyst. These results, predicted using the *DMRA*, are in agreement with the fact that neither the original activity nor the catalyst surface can be restored after regeneration in H_2. Instead, a clean surface, with similar characteristics to that of the fresh catalyst, seems to be re-established after regeneration in air. Even more, the higher initial conversion predicted after regeneration in air may be indicative of some surface structure reorganization [16].

The *DMRA* developed for integral reactor, Eqs. (1)–(11), was applied to fit the experimental data obtained with the fresh catalyst in the whole temperature range of 170–220 °C. First of all, the experimental values corresponding to each temperature were fitted using a monovariable analysis. A satisfactory fitting for each set of experimental data was obtained (Fig. 4). All the estimates for the intrinsic kinetic constants were significantly different from zero within a confidence level of 95% (Table 2). Besides, it was observed that when the reaction temperature increases, the kinetic constant estimates for the main reaction increased one order of magnitude. Instead, the kinetic constant estimates for deactivation and regeneration increase only by a factor of 2 in both cases. A satisfactory linear correlation was obtained when each kinetic parameter, in logarithmic scale, was represented against the temperature reciprocal (Fig. 7). This is indicating that Arrhenius law is valid for the system studied in this work.

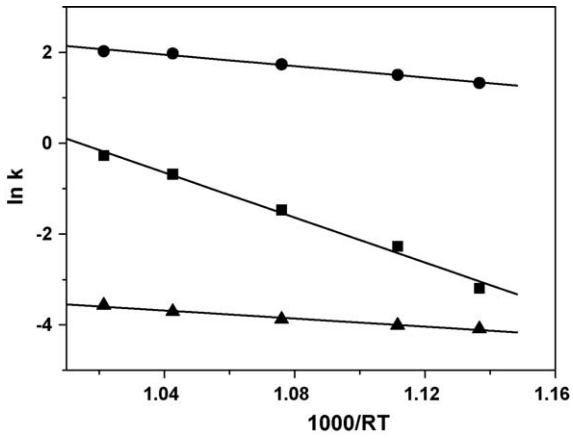

Fig. 7. Arrhenius plot for k_{MA} (■), k_d (●) and k_r (▲) parameters.

From a multivariable analysis and applying the *DMRA* for integral reactor, Eqs. (1)–(11), the apparent activation energies for each step were estimated. The values obtained for these apparent activation energies were: 33.4 kcal/mol for the main reaction, 12.1 kcal/mol for the deactivation step and 6.1 kcal/mol for the regeneration step (Table 3). The low values of apparent activation energies for the deactivation and regeneration steps may be indicating that these two processes are strongly depending on the adsorption and desorption of the deactivating species, which results in a weak net effect of temperature. On the other hand, estimates of 1.7 for n_1 (order respect to *MA* for the hydrogenation reaction, Eq. (6)) and 0.86 for n_d (order respect to *MA* in the deactivation function, Eq. (8)) were obtained in this multivariable analysis (Table 3). It is worth to note that the best fitting with experimental data for fresh catalyst, considering differential reactor, was obtained for m = 2 and h = 1. These integer values are close to the estimates calculated for n_1 = 1.7 and n_d = 0.86. As it was mentioned above, the physical meaning of m is the number of active sites involved in the controlling step of the *MA* hydrogenation. Taking into account that in all of the experiments the main product of reaction was *SA* and just very small amounts of *GBL* were detected, we may consider that the main reaction was the hydrogenation of *MA* into *SA*. Then, the controlling step of the

Table 2
Kinetic and statistical parameters obtained considering integral reactor with monovariable fitting (T = 170–220 °C, W/F^0_{MA} = 11.9 g cat. h/mol *MA*, P = 1 bar).

T (°C)	k_{MA} ± c.i. (mol *MA* g^{-1} min^{-1} atm$^{-1.6}$)	k_d ± c.i. (min^{-1} atm$^{-0.86}$)	k_r ± c.i. (min^{-1})
170	0.0411 ± 0.0006	3.7722 ± 0.1734	0.0168 ± 0.0014
180	0.1033 ± 0.0016	4.4994 ± 0.1808	0.0182 ± 0.0012
195	0.2305 ± 0.0032	5.6954 ± 0.3641	0.0207 ± 0.0007
210	0.5065 ± 0.0069	7.2231 ± 0.1617	0.0245 ± 0.0007
220	0.7626 ± 0.0134	7.6045 ± 0.2497	0.0283 ± 0.0007

c.i.: confidence interval within a 95%.

Table 3
Kinetic and statistical parameters obtained considering integral reactor with multivariable fitting (T = 170–220 °C, W/F^0_{MA} = 11.9 g cat. h/mol *MA*, P = 1 bar).

Parameter	Estimates	c.i. (95%)
k_{MA} (mol *MA* g^{-1} min^{-1} atm$^{-1.6}$)*	0.258	0.027
k_d (min^{-1} atm$^{-0.86}$)*	3.74	0.46
k_r (min^{-1})*	0.0202	0.008
n_1	1.7	0.56
n_d	0.86	0.28
E_a (kcal/mol)	33.5	1.6
E_d (kcal/mol)	12.1	0.9
E_r (kcal/mol)	6.1	1.1

* Estimated at T_m = 195 °C; c.i.: confidence interval within a 95%.

main reaction would be the hydrogenation of *MA* adsorbed on two metal copper sites. Thus, it is not surprising that n_1 is approximately equal to m. In a similar way, the physical meaning of h is the number of active sites involved in the controlling step of the deactivation reaction. If it is assumed that the main cause of deactivation was strong adsorption of *MA* on one metal copper site [32], the similarity between n_d and h may be also explained.

The results obtained in this work show that *Cu/SiO$_2$* catalyst is deactivated during the gas-phase hydrogenation of *MA*. Reactant conversion drops until a residual activity was reached. Various deactivation causes may be invoked: (a) deactivation by the carbon deposition formed during the reaction; (b) deactivation by very strong adsorption of reactant (*MA*) and/or main product (*SA*); (c) deactivation by sintering of the accessible metallic fraction. Sintering is quite unlikely to have an important influence because: (1) the starting catalyst has a very low metallic dispersion; (2) the reaction temperature is not high enough to produce the metallic fraction sintering. Besides, on the basis of results obtained by TPO and in the regeneration experiments, the main cause for catalyst deactivation seems to be reversible deposition of some carbonaceous species. Regeneration under oxidizing atmosphere allowed the recovering of the catalyst initial activity. Moreover, the *DMRA* predicts that the initial activity of regenerated catalysts is some higher than that of fresh catalyst. Instead, hydrogen treatment results in a not effective process for regeneration because the initial conversion is lower than with fresh catalyst. On the other hand, for the fresh catalyst and the catalyst regenerated in an oxidizing stream, the kinetic orders respect to *MA* for the main and the deactivation reactions were 2 and 1, respectively. These two values are quite similar to those estimated for n_1 and n_d. This may be interpreted as if two metallic sites are involved in the controlling step of the main reaction and only one active site in the deactivation reaction [30,31]. Instead, for the catalyst regenerated in a reductive stream, the corresponding kinetic orders, m and h, were equal to two for both reactions. Then, two active sites seem to be involved on the controlling step of both the main reaction and the deactivation reaction.

Taking into account the metal surface heterogeneity of large copper particles and the kinetic orders estimated applying the *DMRA* used in this work, we proposed that the *MA* molecule can interact in at least two different ways with metal copper surface. Depending on the type of interaction, *MA* can be hydrogenated selectively to *SA* or give some type of coke precursor. If *MA* interacts simultaneously with two metal copper sites ($m = 2$), in such a way that C=C bond is preferentially activated, then it can be hydrogenated to *SA*. Then, *SA* will be rapidly desorbed from the metal surface. In other words, it is assumed that *SA* interacts very weakly with metal copper surface. This is in agreement with the low conversion of *SA* into *GBL* observed in this work with Cu(10%)/SiO_2. If *MA* is very strongly adsorbed on metal copper site, some coke precursor can be formed and the number of active sites will be reduced. This last reaction would be much slower than *MA* hydrogenation into *SA* and it is strongly depending on the adsorption step. This is in agreement with: (1) the low amount of carbon compounds deposited on the copper surface; (2) the low apparent activation energy predicted by the *DMRA* fitting. According to the *DMRA* kinetic modeling, the deactivation reaction on fresh catalyst and on catalyst regenerated in air flow seems to start by very strong adsorption of *MA* on one active site ($h = 1$). Furthermore, if some of these strongly adsorbed species react with hydrogen, additional *SA* and some small amounts of *GBL* can be formed. This last process is explaining the partial catalyst regeneration predicted by the *DMRA* during gas-phase *MA* hydrogenation over Cu(10%)/SiO_2. Some of the more strongly adsorbed *MA* and/or coke precursor, which cannot be desorbed in the reaction conditions used in this work, is removed by treatment in H_2 flow at 300 °C. However, part of the carbonaceous residues cannot be removed by this treatment and remains on the metal surface. Moreover, part of this carbonaceous deposit seems to react with hydrogen to form a more stable coke precursor (Fig. 6, curve b). This is modifying the metal copper surface in such a way that now the deactivation occurs by interaction of *MA* molecules with two active sites of the metal copper surface ($h = 2$). In summary, the results obtained with the *DMRA* may be interpreted considering a change in the deactivation mechanism when some coke residues remain on the catalyst surface after treatment in H_2 at 300 °C. Only the treatment in air at 300 °C is able to remove all the carbonaceous deposits formed during gas-phase *MA* hydrogenation on Cu(10%)/SiO_2 and re-established the original metal copper surface Then, the *DMRA* is predicting same behavior for fresh catalyst and catalyst regenerated in oxidizing atmosphere ($m = h = 1$). In summary, regeneration under oxidizing atmosphere allows the almost complete removal of carbonaceous deposits and probably also induces some surface reconstruction [16,29].

4. Conclusions

Cu/SiO_2 catalyst is highly selective to succinic anhydride in the gas-phase hydrogenation of maleic anhydride. However, this copper-based catalyst suffers a rapid deactivation during reaction. This deactivation was initially attributed to carbonaceous compounds deposited on the metal copper surface. The original activity of the copper-based catalyst can be re-established by treatment in oxidant atmosphere. Even more, an increase in the initial conversion seems to be obtained, which may be attributed to a surface reconstruction of metal copper crystallites. On the contrary, only a partial recovery of the initial catalytic activity can be reach after treatment in reductive atmosphere. In all cases, a residual activity, which depends on the experimental conditions, was reached during *MA* hydrogenation in gas phase.

A deactivation kinetic model with residual activity (*DMRA*), which assumes a reversible deactivation-regeneration process during reaction, was able to interpret the evolution of catalyst activity with time. This model can also predict the increase in initial activity after regeneration in air stream. Furthermore, for fresh catalyst and after regeneration in air, the results obtained from this kinetic modeling are suggesting that the main reaction and the deactivation process are involving a different number of active sites. In other words, these two steps seem to occur by different and parallel mechanisms. It was suggested that maleic anhydride is absorbed over two metal copper sites to be then hydrogenated into succinic anhydride. Instead, deactivation starts from maleic anhydride strongly adsorbed over one metal copper site. After regeneration in hydrogen stream, the model predicts a change in the deactivation process. This change may be due to the presence of remaining carbon residues that modifies the metal copper surface.

Acknowledgments

We thank the Universidad Nacional del Litoral (UNL), Consejo Nacional de Investigaciones Científicas y Técnicas (CONICET) and Agencia Nacional de Promoción Científica y Tecnológica (ANPCyT), Argentina for the financial support of this work.

References

[1] M. Messori, A. Vaccari, J. Catal. 150 (1994) 177.
[2] R. Zhang, H. Yin, D. Zhang, L. Qi, H. Lu, Y. Shen, T. Jiang, Chem. Eng. J. 140 (2008) 488.
[3] U.R. Pillai, E. Sahle-Demessie, D. Young, Appl. Catal. B: Environ. 43 (2003) 131.
[4] G. Budroni, A. Corma, J. Catal. 257 (2008) 403.
[5] G.L. Castiglioni, Appl. Catal. A 123 (1995) 144.

[6] G.L. Castiglioni, C. Fumagalli, R. Lancia, M. Messori, A. Vaccari, Chem. Ind. (London) 13 (1993) 510.
[7] Y.L. Zhu, J. Yang, G.Q. Dong, H.Y. Zheng, H.H. Zhang, H.W. Xiang, Y.W. Li, Appl. Catal. B: Environ. 57 (2005) 183.
[8] H. Jeong, T.H. Kim, K.I. Kim, S.H. Cho, Fuel Proc. Technol. 87 (2006) 497.
[9] S.M. Jung, E. Godard, S.Y. Jung, K.C. Park, J.U. Choi, Catal. Today 87 (2003) 171.
[10] S.H. Vaidya, C.V. Rode, R.V. Chaudahari, Catal. Commun. 8 (2007) 340.
[11] R.V. Chaudahari, C.V. Rode, R.M. Deshpande, R. Jaganathan, T.M. Leib, P.L. Mills, Chem. Eng. Sci. 58 (2003) 627.
[12] Y. Hara, H. Kusaka, H. Inagaki, K. Takahashi, K. Wada, J. Catal. 194 (2000) 188.
[13] S.M. Jung, E. Godard, S.Y. Jung, K.C. Park, J.U. Choi, J. Mol. Catal. A: Chem. 198 (2003) 297.
[14] W. Lu, G. Lu, Y. Guo, Y. Guo, Y. Wang, Catal. Commun. 4 (2003) 177.
[15] C. Ohlinger, B. Kraushaar-Czarnetzki, Chem. Eng. Sci. 58 (2003) 1453.
[16] A.J. Marchi, J.L.G. Fierro, J. Santamaría, A. Monzon, Appl. Catal. 142 (1996) 375.
[17] G.A. Fuentes, Appl. Catal. 15 (1985) 33.
[18] R. Christoph, M. Baerns, Chem. Ing. Tech. 57 (1985) 775.
[19] L.R. Radovic, M.A. Vannice, Appl. Catal. 29 (1987) 1.
[20] J. Corella, J. Adanez, A. Monzón, Ind. Eng. Chem. Res. 27 (1988) 375.
[21] C.H. Bartholomew, Appl. Catal. 107 (1993) 1.
[22] A. Borgna, E. Romeo, A. Monzón, Chem. Eng. J. 94 (2003) 19.
[23] A. Borgna, J. Sepúlveda, S.I. Magni, C.R. Apesteguía, Appl. Catal. A: Gen. 276 (2004) 207.
[24] N.M. Ostrovskii, Chem. Eng. J. 120 (2006) 73.
[25] A. Monzón, T. Garetto, A. Borgna, Appl. Catal. A: Gen. 248 (2003) 279.
[26] A. Borgna, T.F. Garetto, A. Monzón, C.R. Apesteguía, J. Catal. 146 (1994) 69.
[27] J.C. Rodríguez, J.A. Peña, A. Monzón, K. Li, R. Hughes, Chem. Eng. J. 58 (1995) 7.
[28] E. Romero, J.C. Rodríguez, J.A. Peña, A. Monzón, Can. J. Chem. Eng. 74 (1996) 1034.
[29] T.F. Garetto, C.I. Vignatti, A. Borgna, A. Monzón, Appl. Catal. B: Environ. 87 (2009) 211.
[30] J. Corella, J.M. Asua, Ind. Eng. Chem. Proc. Des. Dev. 21 (1982) 55.
[31] M.A. Vannice, Kinetics of Catalytic Reactions, Springer Science + Business Media, Inc., New York, USA, 2005, pp. 191–192.
[32] M. Boudart, Michel, G. Djega-Mariadassou, Kinetics of Heterogeneous Catalytic Reactions, Princeton Univ. Press, Princeton, New Jersey, USA, 1984 (Chapter 3).